Chaperon-mediated autophagy can promote proliferation and invasion of renal carcinoma cells and inhibit apoptosis through PKM2

SHANGWEN XIAO[1], GANG XU[2], ZHENLONG WANG[3] and TIE CHONG[3]

[1]Xi'an Jiaotong University, Xi'an, Shaanxi 710061; [2]Department of Urology, Ankang Hospital of Traditional Chinese Medicine, Ankang, Shaanxi 72500; [3]Department of Urology, The Second Affiliated Hospital of Xi'an Jiaotong University, Xi'an, Shaanxi 710004, P.R. China

Received November 16, 2020; Accepted May 21, 2021

DOI: 10.3892/or.2021.8165

Abstract. The aim of the present study was to explore the effect of chaperon-mediated autophagy (CMA) through pyruvate kinase isoform M2 (PKM2) on the development of renal carcinoma (RCC) and its possible mechanisms. Lysosome-associated membrane protein 2A (LAMP-2A) and PKM2 expression levels were detected by collecting tissue samples from RCC patients. RNA interference was used to silence the LAMP-2A and PKM2 expression levels in renal cell line A498 to detect the proliferation, apoptosis and invasion of cells. The levels of mRNA and protein of related genes were also examined. Co-immunoprecipitation was used to detect the interaction between PKM2 and heat shock cognate 70 (HSC70). The results revealed that LAMP-2A and PKM2 expression levels were significantly increased in RCC tissues and cell lines ($P<0.01$). LAMP-2A silencing increased the expression level of PKM2 in A498 and 786-O cells. LAMP-2A and PKM2 silencing suppressed the proliferation and invasion and induced the apoptosis of A498 cells, and also affected the expression levels of related genes. Co-immunoprecipitation revealed the interaction between PKM2 and HSC70. In conclusion, CMA could affect the proliferation, invasion and apoptosis of RCC cells through PKM2, and our findings provided new biomarkers and targets for molecular targeted therapy of RCC.

Correspondence to: Dr Tie Chong or Dr Zhenlong Wang, Department of Urology, The Second Affiliated Hospital of Xi'an Jiaotong University, 157 West 5th Yanta Road, Xi'an, Shaanxi 710004, P.R. China
E-mail: chongtie@126.com
E-mail: zhenlongw2001@xjtu.edu.cn

Key words: chaperon-mediated autophagy, pyruvate kinase isoform M2, renal carcinoma

Introduction

There are three forms of autophagy, including chaperone-mediated autophagy (CMA), which is a process of recognizing proteins with the KFERQ sequence through HSC70 and sending them to the surface of lysosome membrane to be combined with lysosome-associated membrane protein 2A (LAMP-2A), a specific CMA protein receptor, to make the protein unfold and then enter the lumen of the lysosome for lysosomal degradation (1,2). As a rate-limiting protein of CMA, LAMP-2A is widely used as a target to block CMA activity (3,4). Kon *et al* determined that the activity of CMA in a variety of cancer cells increased, and LAMP-2A expression was upregulated, demonstrating that CMA is a necessary condition for malignant cell growth and tumor metastasis (5). Through the study of 593 gastric non-cancerous foci and 173 gastric cancer tissues, LAMP-2A was revealed to be a potential biomarker for early prediction and prognosis of gastric cancer (6).

Tumor cells rely mainly on aerobic glycolysis to produce ATP, which in the case of adequate oxygen supply leads to increased glucose uptake and lactic acid production compared with normal cells, a phenomenon known as the Warburg effect (7). Activation of oncogenes or deletion of anti-oncogenes increase glucose uptake and lactate production. During oncogenesis, the expression of pyruvate kinase continues to change, which is a key glycolytic enzyme (8,9) that catalyzes the transfer of phosphate from phosphoenolpyruvate (PEP) to ADP, leading to the formation of pyruvate and ATP. Cancer cells commonly express the M2 isoform of embryonic pyruvate kinase (PKM2), which may contribute to the transition of metabolism from oxidative phosphorylation to aerobic glycolysis and tumor formation (10,11). Previous research has demonstrated that PKM2 could be a potential target for tumor regulation (12). A previous study revealed that the acetylation of PKM2 K305 promoted its lysosomal-dependent degradation through CMA, increased the interaction between PKM2 and CMA chaperone HSC70, and promoted cell proliferation and tumor growth (13).

However, the specific mechanism of action of CMA and PKM2 in RCC has yet to be reported. Based on this, the present study investigated the effect of CMA and PKM2 on the

development of renal cancer (RC) and its possible mechanism of action.

Materials and methods

Tissues and cell lines. The tumor tissues and paired para-cancer (PC) tissue samples (margins of tumor tissues 3 cm) were collected from 12 patients who underwent surgery for RC at the Second Affiliated Hospital of Xi'an Jiaotong University (Xi'an, China) from January to December 2019. The inclusion criteria was as follows: Patients who were diagnosed with renal cancer by abdominal CT and postoperative pathological examination; in line with the indications of surgical treatment; complete clinical data; patients and their family members were informed of this study and signed informed consent. The exclusion criteria was as follows: hypertension, diabetes mellitus, kidney disease, adrenal disease and hepatic and renal insufficiency; people with coagulation dysfunction; confused patients; poor compliance; women who were lactating or pregnant. The study included 9 male and 3 female patients, with a mean age of 54.7 years (range from 42 to 71 years). All of the included patients were informed of the study and signed an informed consent. Our study was approved by the Ethics Committee of the Second Affiliated Hospital of Xi'an Jiaotong University, Xi'an, China.

Human normal renal cells HK-2 and human RCC cell lines A498, GRC-1, 786-O and ACHN were purchased from the Cell Bank of the Shanghai Institute of Biochemistry and Cell Biology, Chinese Academy of Sciences. These cells were cultured in RPMI-1640 medium (Thermo Fisher Scientific, Inc.) supplemented with 10% fetal bovine serum (FBS; Gibco; Thermo Fisher Scientific, Inc.) in an incubator containing 5% CO_2 at 37˚C.

Cell transfection. The cDNA of LAMP-2A and PKM2 were amplified using RNA extracted from 293T cells (Cell Bank of the Shanghai Institute of Biochemistry and Cell Biology, Chinese Academy of Sciences). After the cells were cultured at 37˚C to the logarithmic growth phase, the cells were inoculated into a 12-well plate, and the cell density was adjusted to $3x10^5$ cells/well. A minimum of two independent shRNAs for LAMP-2A or PKM2 were designed, synthesized and packaged by Guangzhou RiboBio Co., Ltd. shRNAs were cloned into a pLKO.1 puro vector (Addgene, Inc.) according to the manufacturer's protocol. The shRNA sequences used are presented in Table I. The second generation of 80% confluent cells were transfected with lentiviral particles (MOI=16), with 15 μg pLKO.1-shRNA-LAMP-2A/PKM2 plasmid or a scrambled sequence using Lipofectamine 3000 (Invitrogen; Thermo Fisher Scientific, Inc.) for 10 min at 20˚C. A total of 72 h after transfection, the cells were harvested. The cells were divided into four groups and transfected with empty control vector (Control), sh-LAMP-2A vector [LAMP-2A(-)], sh-PKM2 vector [PKM2(-)], and sh-LAMP-2A + sh-PKM2 vectors [LAMP-2A(-) PKM2(-)].

Reverse transcription-quantitative (RT-q) PCR. RT-qPCR was performed using the SYBR-Green PCR Master Mix according to the manufacturer's instructions with an ABI 7300HT RT-PCR system (Applied Biosystems; Thermo Fisher Scientific, Inc.) to determine the expression level of related mRNA. After extracting the total RNA from cells or tissue with the TRizol reagent (Invitrogen; Thermo Fisher Scientific, Inc.), the cDNA was synthesized by reverse transcription experiment using a reverse transcription synthesis kit (PrimeScript™ RT reagent kit; Takara Bio, Inc.) with Oligo dT primer, Prime Script Buffer and dNTP according to the manufacturer's instructions. GAPDH was used as an internal reference. The primer sequences used are presented in Table II. The thermocycling conditions were as follows: 95˚C for 8 min, 1 cycle; 95˚C for 25 sec, 64˚C for 20 sec; 72˚C for 20 sec, 10 cycles; 93˚C for 25 sec, 60˚C for 35 sec, and 72˚C for 20 sec, 35 cycles. The relative expression level of related genes was calculated using the $2^{-\Delta\Delta Cq}$ method (14). $\Delta\Delta$Cq=[Cq target gene (sample)-Cq GAPDH (sample)]-[Cq target gene (calibration sample)-Cq GAPDH (calibration sample)].

Western blot analysis. Cells or tissues were collected and lysed with RIPA cleavage buffer (Thermo Fisher Scientific, Inc.). The protein concentration was quantified with BCA reagent (Thermo Fisher Scientific, Inc.). Then, 250 μg proteins were separated by electrophoresis in 10% SDS-PAGE and transferred to nitrocellulose membranes (EMD Millipore). The membranes were blocked in 5% BSA at 37˚C for 2 h and then incubated with a primary antibody at 4˚C overnight. After washing with TBST (1% Tween-20), the membranes were incubated with a secondary antibody (goat anti-rabbit IgG HRP; 1:3,000 dilution; product code ab205718; Abcam) for 2 h at room temperature. The membranes were visualized with an ECL kit (Thermo Fisher Scientific, Inc.), and finally the band density on the membrane was scanned and analyzed using an image analyzer (model no. MSD910) with Biomaster analysis software (both from Beijing Maisiqi High Technology Co., Ltd.).

The following primary antibodies were used: anti-LAMP-2A (1:1,000 dilution; product code ab125068; Abcam), anti-PKM2 (1:1,000 dilution; product no. 4053; Cell Signaling Technology, Inc.), anti-proliferating cell nuclear antigen (PCNA) (1:1,000 dilution; product code ab92552), anti-hypoxia inducible factor (HIF)-1 (1:1,000 dilution; product code ab179483), anti-p21 (1:1,000 dilution; product code ab109199), anti-vascular endothelial growth factor (VEGF) (1:1,000 dilution; product code ab150375), anti-cleaved caspase-3 (1:1,000 dilution; product code ab32042), anti-Bcl-2 (1:1,000 dilution; product code ab32124), anti-Bax (1:1,000 dilution; product code ab182733) and anti-GAPDH (1:2,000 dilution; product code ab8245; all from Abcam).

Cell proliferation assay. The proliferation level of A498 cells was detected by CCK-8 kit (Beyotime Biotechnology), and the experiment was carried out according to the manufacturer's instructions. Briefly, the cells were inoculated in 96-well plates with an inoculation density of $5x10^3$ cells/well. The cells were cultured at 37˚C for 48 h and 10 μl of CCK-8 reagent was added to each well. After incubation for 1 h, the absorbance at 450 nm was measured with a microplate reader. The results were representative of three independent experiments.

Cell cycle and apoptosis analysis. After transfection, cells ($1x10^5$ per well) were collected, prepared into single-cell

Table I. Sequences of shRNA used in the experiments.

Gene	Sequence
LAMP-2A	5'-CACCGCACCATCATGCTGGATATGACGAATCATATCCAGCATGATGGTGC-3'
	3'-CGTGGTAGTACGACCTATACTGCTTAGTATAGGTCGTACTACCACGAAAA-5'
PKM2	5'-CCGGCGGGTGAACTTTGCCATGAATTTCAAGAGAATTCATGGCAAAGTTCA
	CCCGTTTTTGGTACC-3'
Scrambled	3'-GCCCACTTGAAACGGTACTTAAAGTTCTCTTAAGTACCGTTTCACGTG
	GGCAAAAAACCATGGTTAA-5'

LAMP-2A, lysosome-associated membrane protein 2A; PKM, pyruvate kinase.

Table II. Primer sequences used in the reverse transcription-quantitative PCR.

Gene	Sequence (5'-3')
LAMP-2A	F: ACAGCTCAAGACTGCAGTGC
	R: ATGATGGTGCTTGAGACCAAT
PKM2	F: CCTTGCAATTATTTGAGGAACTCCGC
	R: CACGGTACAGGTGGGCCTGAC
PCNA	F: GACTCGTCTCATGTCTCTTTGGTG
	R: GTATTTTGGACATGCTGGTGAGG
VEGF	F: GAAGTTCATGGATGTCTATCAGCG
	R: ACTCCGTCAGAACTATCAAAGCTGC
HIF-1	F: TAAAGGAATTTCAATATTTGATGGG
	R: AAAGGGTAAAGAACAAAACACACAG
p21	F: GCCACTGTGATGCGCTAATG
	R: AGAAGATCAGCCGGCTAATG
Bcl-2	F: GTGGAGGAGCTCTTCAGGGA
	R: AGGCACCCAGGGTGATGCAA
Bax	F: GGCC-CACCAGCTCTGAGCAGA
	R: GCCACGTGGGGGTCCCAAAGT
Cleaved	F: CATGGAAGCGAATCAATGGACT
caspase-3	R: CTGTACCAGACCGAGATGTCA
GAPDH	F: AAGGAGGCGGAGAAGAGGAC
	R: CGTCGTTACGAGTCACTTCAGG

F, forward; R, reverse; LAMP-2A, lysosome-associated membrane protein 2A; PKM, pyruvate kinase; PCNA, proliferating cell nuclear antigen; VEGF, vascular endothelial growth factor; HIF, hypoxia inducible factor.

suspension, washed twice with PBS, and fixed with 70% ethanol at 4˚C overnight. According to the manufacturer's instructions, 1 μl propidium iodide (PI; Thermo Fisher Scientific, Inc.) was added and placed in the dark at 37˚C for 30 min. The cell cycle of each group was detected by flow cytometry (FACSCanto II; BD Biosciences) with FlowJo VX 10 software (FlowJo, LLC), and the proportion of cells in the G1, S and G2 phases was counted.

Cells were collected by the same method without ethanol fixation. A total of 2.5 μl Annexin V-fluorescein isothiocyanate (FITC)/propidium iodide (PI) were added into the cell suspension according to the manufacturer's instructions, and placed in the dark at 37˚C for 15 min. Cell apoptosis was detected by flow cytometry in each group, and early apoptotic cells, late apoptotic cells and dead cells were counted.

Transwell migration assay. Matrigel was diluted with 0.5% FBS in DMEM (Gibco; Thermo Fisher Scientific, Inc.) medium at 1:5 and seeded on the upper surface of the bottom membrane of a 24-mm Transwell chamber (8-μm pore size; Corning, Inc.) for 16 h at 37˚C. Then the cells were incubated for 4 h at 37˚C in an incubator with 5% CO_2. Cells were further cultured in 5% FBS medium for 24 h at 37˚C. After cell counting, the cells were seeded on the upper chamber at $3x10^4$ cells/well. Transwell chambers were fixed with 4% methanol at room temperature for 30 min and stained with 0.1% crystal violet for 20 min at room temperature. A total of 700 μl of culture medium containing 20% calf serum (Gibco; Thermo Fisher Scientific, Inc.) was added in the lower chamber, and the cells were cultured in an incubator at 37˚C in an atmosphere containing 5% CO_2 for 72 h. Five fields were randomly selected under a low-power microscope (magnification x10; Olympus Corporation) for each group to compare the differences in the number of transmembrane cells between the groups.

Immunofluorescence. Cells were fixed with 4% methanol at room temperature for 30 min and permeabilized with 0.1% Triton X-100 in PBS for 20 min. The cells were incubated with anti-PKM2 (1:1,000 dilution; product no. 4053; Cell Signaling Technology, Inc.) and anti-HSC70 (1:1,000 dilution; product code ab223356; Abcam) primary antibodies overnight at 4˚C, and then incubated in fluorochrome-conjugated secondary antibodies goat anti-rabbit IgG (cat. no. A-31556) and donkey anti-mouse IgG (cat. no. Q22082; both 1:2,000 dilution; both Thermo Fisher Scientific, Inc.) for 2 h at room temperature. DAPI was used to counterstain the cell nuclei at 37˚C for 30 min. Images were captured with a laser confocal microscope (Olympus Corporation) in five different fields for each sample.

Co-immunoprecipitation analysis. Approximately $5x10^6$ cells were collected 48 h after transfection and lysed in 0.5 ml RIPA buffer (Beyotime Biotechnology) and centrifuged at 1,000 x g at 4˚C for 10 min. Total cell proteins were extracted as Input

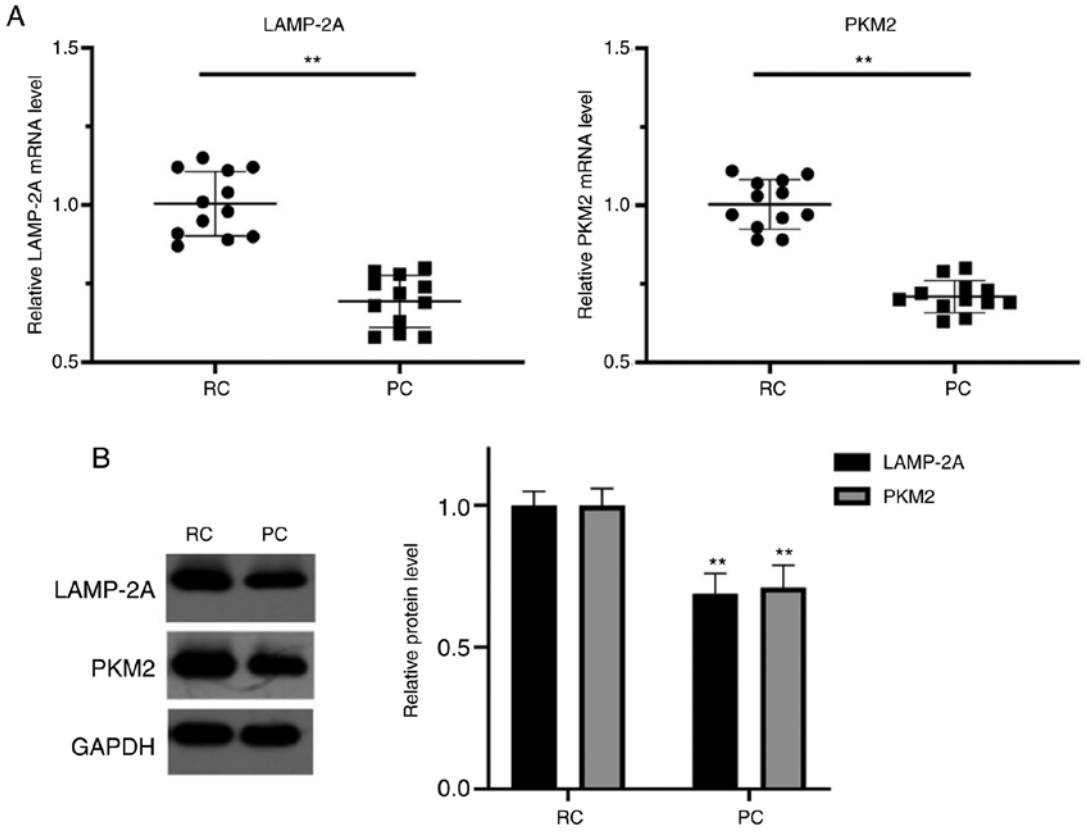

Figure 1. mRNA and protein expression levels of LAMP-2A and PKM2 in RCC tissues are significantly increased. (A) Comparison of mRNA levels of the LAMP-2A and PKM2 in RC tissues and its paired PC tissues. (B) Sample diagram of blots and comparison of the protein levels of LAMP-2A and PKM2 in RC and PC. **P<0.01, compared with PC. LAMP-2A, lysosome-associated membrane protein 2A; PKM, pyruvate kinase; RCC, renal carcinoma; PC, para-cancer; RC, renal cancer.

controls. The precleared lysates (500 μg) were immunoprecipitated against the epitopes with 20 μl of protein A/G-agarose beads (Santa Cruz Biotechnology, Inc.) and incubated with anti-PKM2 antibody (1:1,000 dilution; product no. 4053; Cell Signaling Technology, Inc.) at 4˚C overnight. The resultant mixtures were centrifuged at 250 x g at 4˚C for 5 min and the supernatants were removed. The pellets were washed three times with PBS and western blotting was performed using an anti-HSC70 antibody (1:1,000 dilution; product code ab223356; Abcam) according to the manufacturer's instructions.

Statistical analysis. Each sample was assessed 3 times and all experiments were performed in triplicate. All data were statistically analyzed and plotted using GraphPad software 8 (GraphPad Software, Inc.). The data were expressed as the mean ± standard deviation (SD). The comparisons between two groups were performed by unpaired Student's t-test or Mann-Whitney U test. Comparisons among more than two groups were performed by ANOVA with Fisher's Least Significant Difference (LSD). P<0.05 was considered to indicate a statistically significant difference.

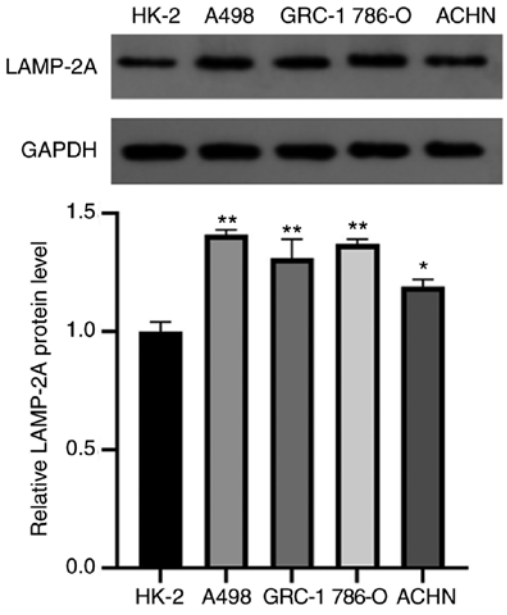

Figure 2. LAMP-2A expression level is significantly increased in renal cancer cell lines. *P<0.05 and **P<0.01, compared with HK-2 cells. LAMP-2A, lysosome-associated membrane protein 2A.

Results

LAMP-2A and PKM2 expression levels are significantly increased in RCC tissues. In the collected tissues of patients that underwent RC surgery at our hospital, the mRNA levels of LAMP-2A and PKM2 were significantly higher in the RC tissues compared with their paired PC tissues (P<0.01), respectively. In addition, the protein levels of LAMP-2A and PKM2 in RC tissues were significantly

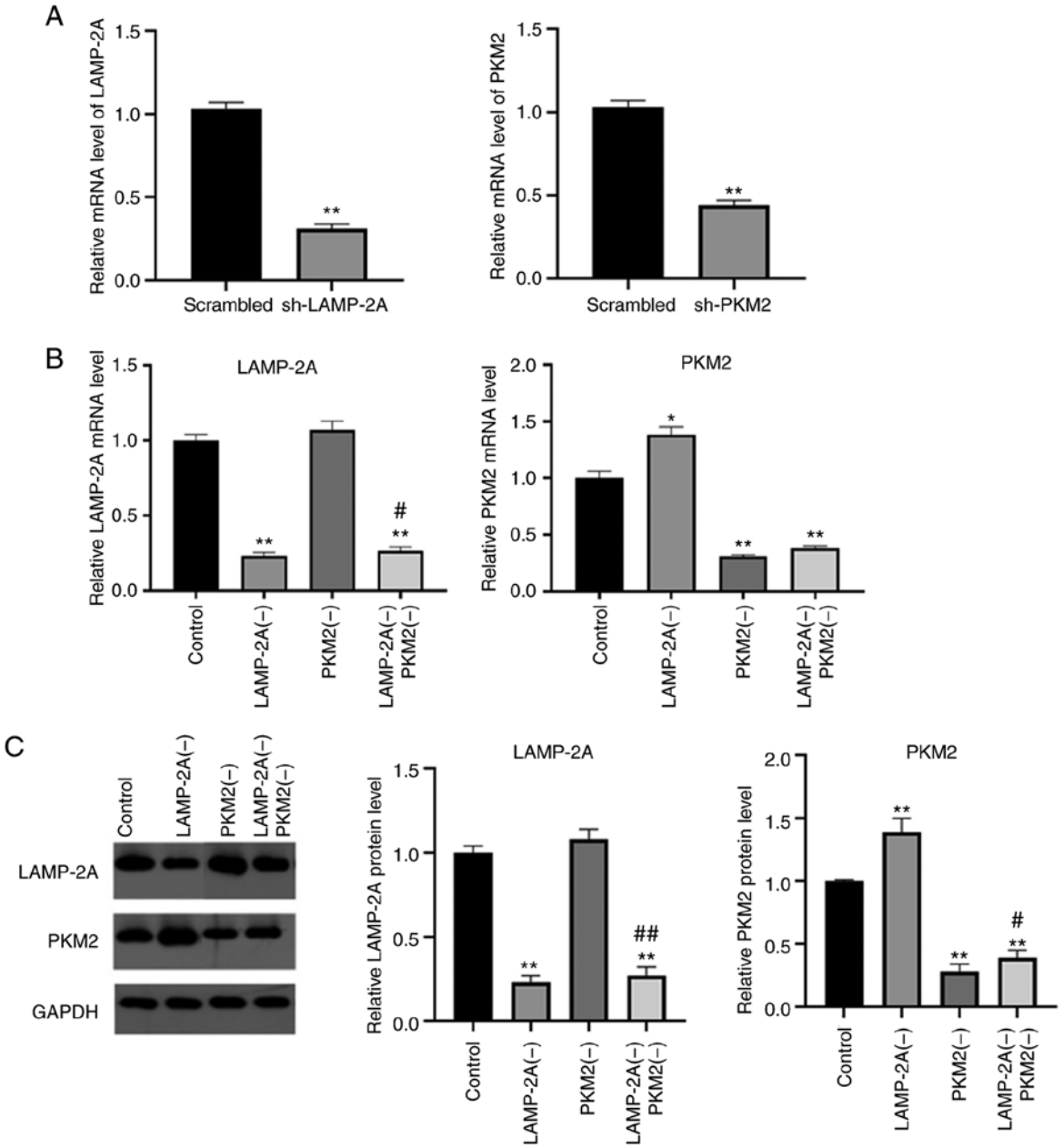

Figure 3. LAMP-2A silencing increases PKM2 mRNA and protein expression levels. (A) The shRNAs effectively knocked down the expression levels of PKM2 and LAMP-2A in A498 cells compared with the scrambled sequence. (B) Comparison of the mRNA levels of LAMP-2A and PKM2 in different groups. (C) Sample diagram of blots and comparison of the protein levels of LAMP-2A and PKM2 in different groups. *P<0.05 and **P<0.01, compared with the Control group; $^{\#}$P<0.05 and $^{\#\#}$P<0.01, compared with the PKM2(-) group. LAMP-2A, lysosome-associated membrane protein 2A; PKM, pyruvate kinase; sh-, short hairpin.

higher than those in their paired PC tissues (P<0.01), respectively (Fig. 1).

Level of LAMP-2A is significantly increased in RCC cell lines. The protein levels of LAMP-2A were assessed in human normal renal cells HK-2 and four RC cell lines: A498, GRC-1, 786-O and ACHN. LAMP-2A expression levels in different cells are revealed in Fig. 2. LAMP-2A expression levels were significantly increased in all four types of RC cells compared with normal renal cells (P<0.05 or P<0.01). Among them, LAMP-2A had the highest relative expression level in A498 cells, and was therefore selected for subsequent experiments.

LAMP-2A silencing increases PKM2 expression level in A498 cells. A498 cells were transfected with shRNAs to knock down the expression levels of PKM2 and LAMP-2A, and the mRNA levels revealed that shRNAs effectively knocked down the expression levels of both genes in A498 cells compared with the scrambled sequences (Fig. 3A). The mRNA and protein levels of LAMP-2A and PKM2 in each group were assessed, and the results are demonstrated in Fig. 3B and C.

LAMP-2A mRNA and protein levels in the LAMP-2A(-) group and LAMP-2A(-) PKM2(-) group were significantly decreased (P<0.01) compared with the Control group, and there was no significant difference between the PKM2(-) group and the Control group (P>0.05).

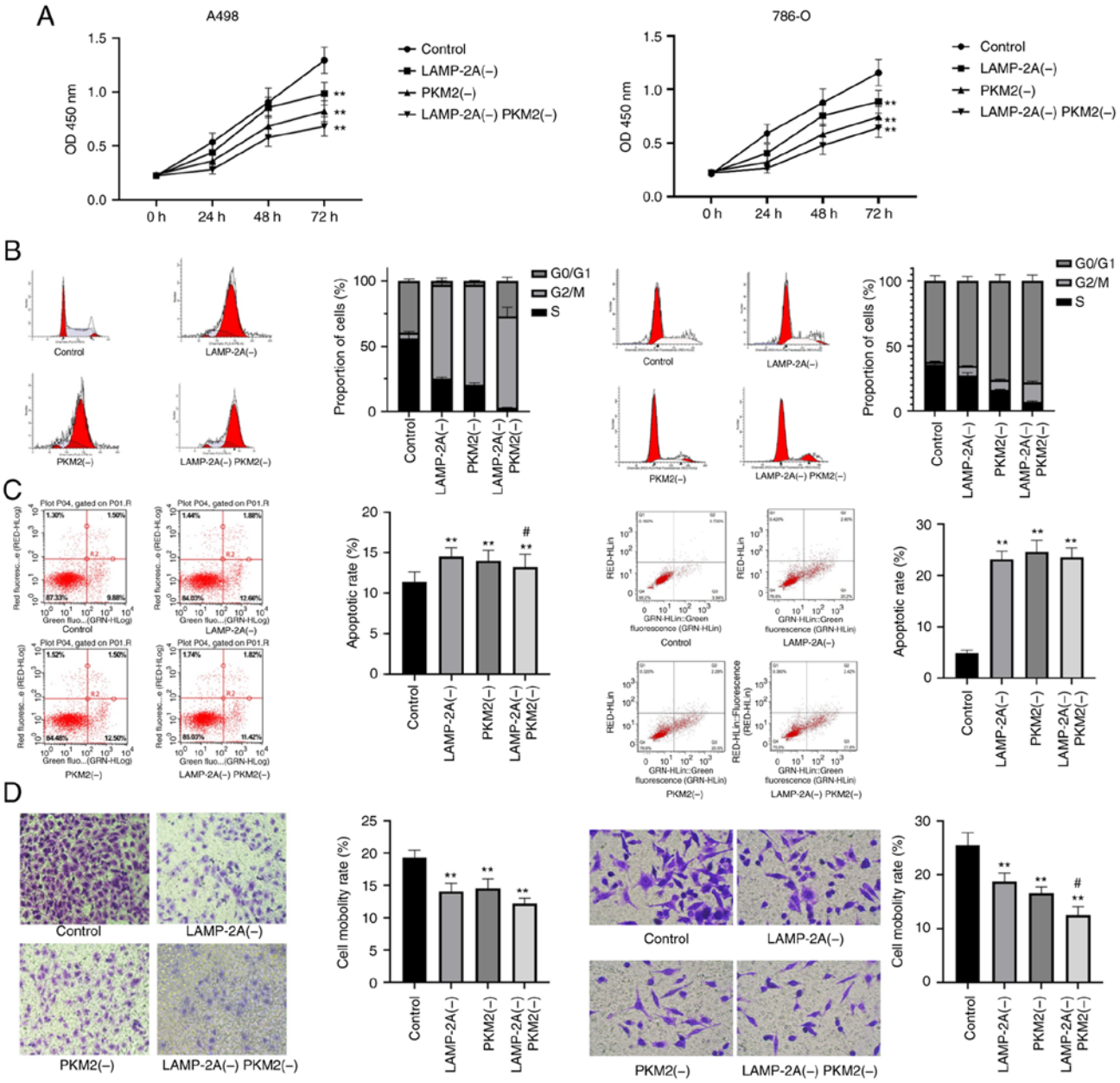

Figure 4. LAMP-2A and PKM2 silencing inhibits proliferation and invasion and induces apoptosis of A498 cells. (A) Cell proliferation in each group was detected by Cell Counting Kit-8. (B) Cell cycle assay results of each group. (C) Apoptosis of cells in each group. (D) Invasive ability of cells in each group. **P<0.01, compared with the Control group; and $^{\#}$P<0.05, compared with the PKM2(-) group. LAMP-2A, lysosome-associated membrane protein 2A; PKM, pyruvate kinase.

The mRNA and protein levels of PKM2 in the PKM2(-) group and LAMP-2A(-) PKM2(-) group were significantly decreased (P<0.01) compared with the Control group. It is worth noting that the mRNA and protein levels of PKM2 were increased in the LAMP-2A(-) group compared with the Control group and the LAMP-2A(-) PKM2(-) group compared with the PKM2(-) group (P<0.05 or P<0.01), indicating that LAMP-2A silencing could reduce the degradation of PKM2.

LAMP-2A and PKM2 silencing suppresses the proliferation and invasion and induces the apoptosis of RCC cells. The proliferation, cell cycle, apoptosis, and invasion of four groups of cells were examined as revealed in Fig. 4. Both LAMP-2A and PKM2 silencing significantly reduced the proliferation rate of A498 and 786-O cells (P<0.01), and the inhibition was greater with their combination. Furthermore, both LAMP-2A and PKM2 silencing significantly promoted the apoptosis of A498 and 786-O cells (P<0.01) and blocked the cell cycle at G2/M phase. In addition, both LAMP-2A and PKM2 silencing significantly inhibited the invasive ability of A498 and 786-O cells (P<0.01), and their combined inhibitory effect was stronger (P<0.05).

LAMP-2A and PKM2 silencing affects the levels of related genes. The levels of mRNA and protein of genes that may be related to CMA and PKM2 were detected (Fig. 5). Compared with the Control group, the mRNA and protein levels of PCNA, VEGF, HIF-1 and the ratio of Bcl-2 to Bax were significantly decreased in the other three groups (P<0.05 or

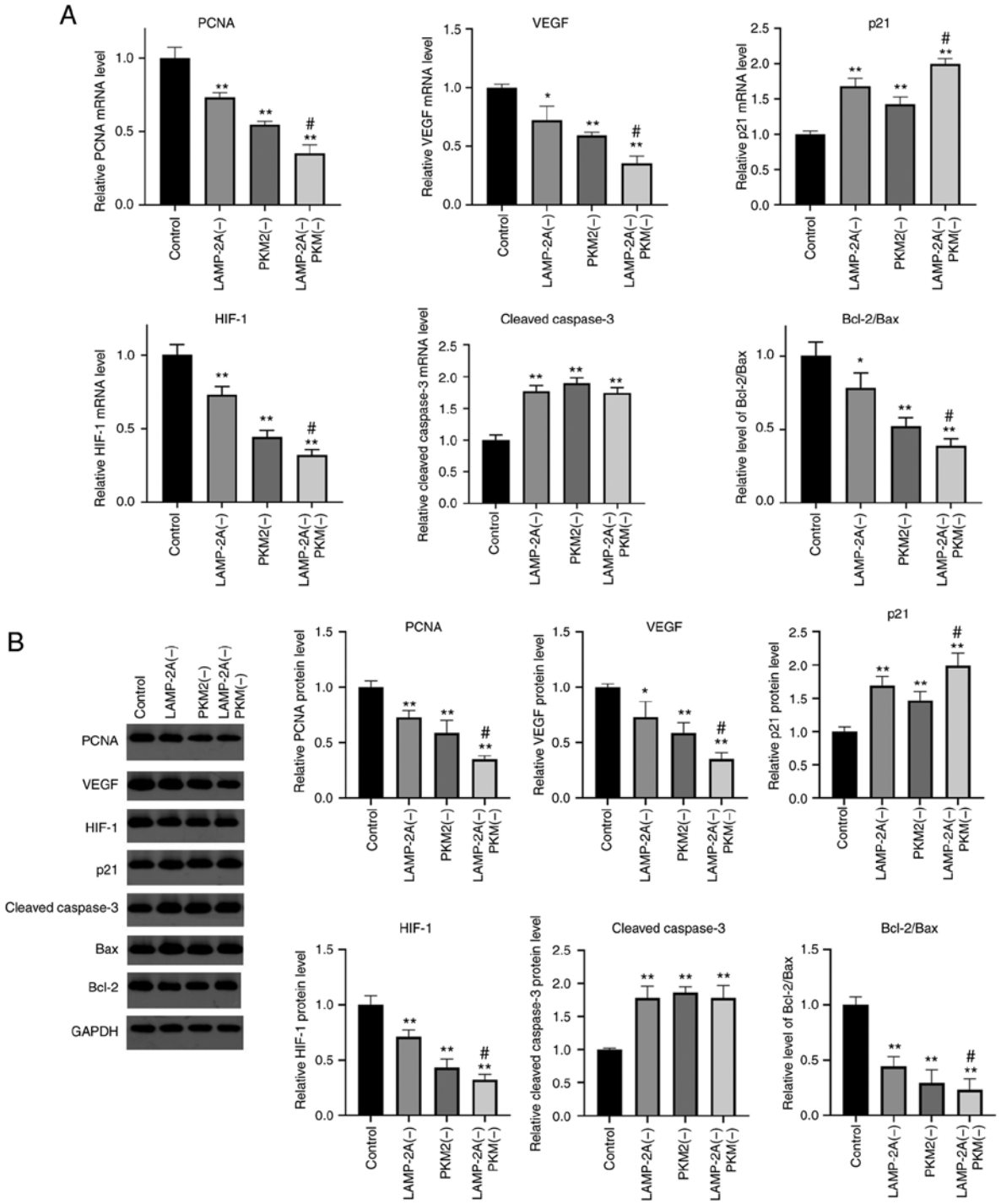

Figure 5. Protein and mRNA expression levels of genes that may be related to CMA and PKM2 are detected. (A) mRNA expression levels of related genes. (B) Protein expression levels of related genes. *P<0.05 and **P<0.01, compared with the Control group; #P<0.05, compared with the PKM2(-) group. LAMP-2A, lysosome-associated membrane protein 2A; PKM, pyruvate kinase; PCNA, proliferating cell nuclear antigen; VEGF, vascular endothelial growth factor; HIF, hypoxia inducible factor.

P<0.01), and the levels of the LAMP-2A(-) PKM2(-) group were significantly lower than that of the PKM2(-) group (P<0.05). The mRNA and protein expression levels of cleaved caspase-3 were significantly higher in the other three groups compared with the Control group (P<0.01). Compared with the Control group, the mRNA and protein expression level of p21 was significantly increased in the other three groups, and the level of the LAMP-2A(-) PKM2(-) group was significantly higher than that of the PKM2(-) group (P<0.05).

Co-immunoprecipitation reveals the interaction between PKM2 and HSC70. The co-immunoprecipitation of PKM2 and HSC70 in each group was also detected, and the results are revealed in Fig. 6B. Immunofluorescence results (Fig. 6A) revealed that PKM2 and HSC70 could co-locate in A498 cells. The interaction between PKM2 and HSC70 was significantly higher in LAMP-2A(-) group than that in PKM2(-) and LAMP-2A(-) PKM2(-) group, with no significant difference from the Control group.

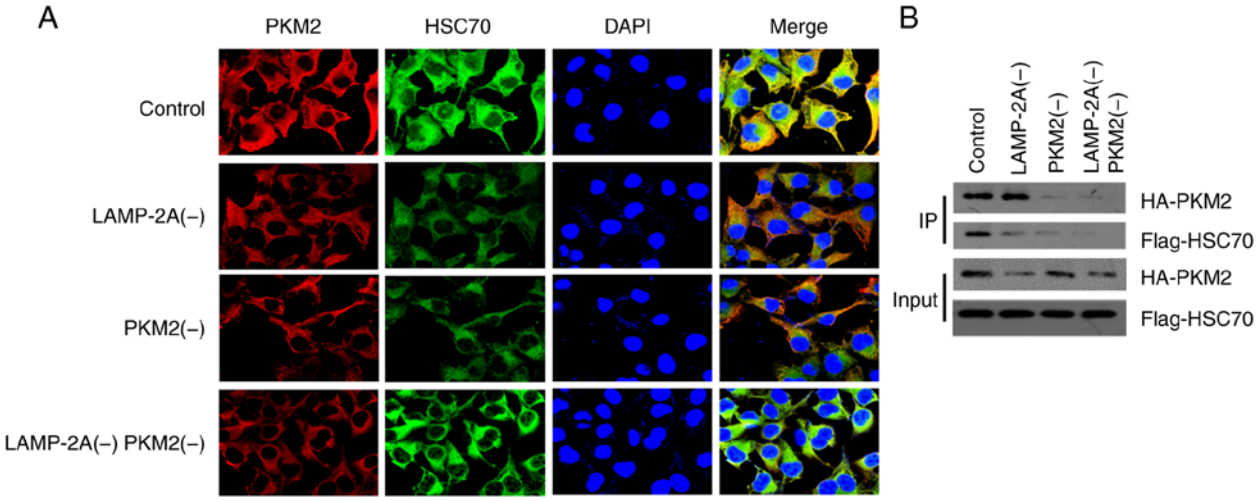

Figure 6. Immunofluorescence results and co-immunoprecipitation of PKM2 and HSC70. (A) Immunofluorescence results revealed that PKM2 and HSC70 could co-locate in A498 cells. (B) Co-immunoprecipitation of PKM2 and HSC70 in each group. PKM, pyruvate kinase; LAMP-2A, lysosome-associated membrane protein 2A.

Discussion

CMA has been revealed to be associated with cancer progression in recent years (15), but its mechanisms have not been fully explored. PKM2 has been reported to be a substrate for CMA in non-small cell lung cancer (13). Knockout of LAMP-2A gene in lung cancer cells indicated that CMA was necessary for proliferation of lung cancer cells (5). In the present study, the mechanism of CMA and PKM2 in the proliferation regulation of RCC was mainly investigated.

In our findings, LAMP-2A and PKM2 expression levels were significantly increased in RCC tissues and cell lines. CMA is considered to play a critical role in a variety of tumors, and PKM2 is also recognized as a regulatory tumor target (16). The results of the present study confirmed that both of them played an equally vital role in the development of RCC.

The acetylation of PKM2 and CMA can promote the degradation of PKM2 (17). The present study revealed that the deletion of LAMP-2A could increase the expression level of PKM2 and reduced the degradation of PKM2 in A498 cells, which is consistent with previous results (17).

Both LAMP-2A and PKM2 silencing significantly reduced the proliferation rate of A498 cells, and this inhibition was greater with their combination. Correspondingly, the expression levels of PCNA, VEGF and HIF-1 were also significantly decreased. The downregulation of PKM2 has been reported to significantly reduce the levels of PCNA, cyclin D1 and p27 in primary astrocytes (18). PKM2 knockdown can lead to impaired cell proliferation and enhanced apoptosis *in vitro* and inhibit tumor growth and decrease angiogenesis *in vivo*. In addition, PKM2 deficiency has been revealed to negatively affect the proliferation chain accumulation and promoter activity of hypoxia-induced HIF-1α, and lead to decreased VEGF secretion (19). The expression and function of PKM2 were closely related to HIF-1 in the feed-forward loop, and HIF-1 was identified as a target gene of the PKM2/STAT3 pathway, and the expression of PKM2 was in turn regulated by the HIF-1 transcription complex (20). Experimental results revealed that inhibition of CMA inhibited the proliferation of colon carcinoma CT26 cells (21). Both CMA blocking and PKM2 knockdown inhibited cell proliferation, and similar results were obtained in the present study with regard to RCC.

Silencing of LAMP-2A and PKM2 promoted apoptosis of A498 cells and blocked the cells in the G2/M phase. Concurrently, the levels of p21 and cleaved caspase-3 were increased while the ratio of Bcl-2/Bax was decreased. In fact, PKM2 has been reported to translocate to the mitochondria, interact with Bcl-2 at threonine 69 site and phosphorylate Bcl-2 to prevent Cul3-based E3 ligase from binding to Bcl-2 and subsequent Bcl-2 degradation, thus directly inhibiting the apoptosis of glioma cells under oxidative stress (22). PKM2 has been revealed to accelerate malignant behavior of colorectal cancer cells, increase oxaliplatin resistance and reduce cell apoptosis (23). A previous study indicated that knockdown of PKM2 blocked the non-small lung cancer cells in the G2/M phase, which was associated with the effect of the expression of p21 (24). PKM2 knockdown activated spindle assembly checkpoints and blocked cell processes during metaphase to anaphase mitosis, leading to apoptosis.

CMA is a substrate protein autophagy substitution pathway, mediated by HSC70 and LAMP-2A. HSC70 recognizes and targets substrate proteins with the KFERQ-like motifs for transport to lysosomal membranes. LAMP-2A assists substrate protein translocation to lysosomes for degradation (25). Co-immunoprecipitation revealed the interaction between PKM2 and HSC70. Acetylation of PKM2 increases its interaction with CMA chaperone HSC70 and accelerates its binding to lysosomes (13). In RCC, CMA and PKM2 may also function in this way.

A limitation of the present study was that *in vivo* experiments were not conducted to verify our conclusions. Therefore, the specific interaction mechanism between CMA and PKM2 still requires further investigation.

In conclusion, the data of the present study supported the hypothesis that CMA affected the proliferation and apoptosis of RCC cells through PKM2, and blockade of CMA or knockdown of PKM2 may be a new treatment strategy for RCC.

Acknowledgements

Not applicable.

Funding

The present study was supported by Xi 'an Science and Technology Planning Project (grant no. 201805096YX4SF30) and the Traditional Chinese Medicine Scientific Research Project of Shaanxi Province (grant no. JCSM038).

Availability of data and materials

The datasets generated and/or analyzed during the present study are available from the corresponding author on reasonable request.

Authors' contributions

SX and TC contributed to the conception and design of the study. GX and ZW performed the experiments, collected and analyzed data. SX and TC wrote the manuscript. All authors reviewed and approved the final version of the manuscript.

Ethics approval and consent to participate

The study protocol was approved by the Ethics Committee of the Second Affiliated Hospital of Xi'an Jiaotong University (Xi'an, China). Written informed consent was obtained from all the study subjects before enrollment.

Patient consent for publication

Not applicable.

Competing interests

The authors declare that they have no competing interests.

References

1. Cuervo AM: Chaperone-mediated autophagy: Selectivity pays off. Trends Endocrinol Metab 21: 142-150, 2010.
2. Agarraberes FA, Terlecky SR and Dice JF: An intralysosomal hsp70 is required for a selective pathway of lysosomal protein degradation. J Cell Biol 137: 825-834, 1997.
3. Park C, Suh Y and Cuervo AM: Regulated degradation of Chk1 by chaperone-mediated autophagy in response to DNA damage. Nat Commun 6: 6823, 2015.
4. Saha T: LAMP2A overexpression in breast tumors promotes cancer cell survival via chaperone-mediated autophagy. Autophagy 8: 1643-1656, 2012.
5. Kon M, Kiffin R, Koga H, Chapochnick J, Macian F, Varticovski L and Cuervo AM: Chaperone-mediated autophagy is required for tumor growth. Sci Transl Med 3: 109ra117, 2011.
6. Zhou J, Yang J, Fan X, Hu S, Zhou F, Dong J, Zhang S, Shang Y, Jiang X, Guo H, *et al*: Chaperone-mediated autophagy regulates proliferation by targeting RND3 in gastric cancer. Autophagy 12: 515-528, 2016.
7. Warburg O: On the origin of cancer cells. Science 123: 309-314, 1956.
8. Altenberg B and Greulich KO: Genes of glycolysis are ubiquitously overexpressed in 24 cancer classes. Genomics 84: 1014-1020, 2004.
9. Majumder PK, Febbo PG, Bikoff R, Berger R, Xue Q, McMahon LM, Manola J, Brugarolas J, McDonnell TJ, Golub TR, *et al*: mTOR inhibition reverses Akt-dependent prostate intraepithelial neoplasia through regulation of apoptotic and HIF-1-dependent pathways. Nat Med 10: 594-601, 2004.
10. Mazurek S, Boschek CB, Hugo F and Eigenbrodt E: Pyruvate kinase type M2 and its role in tumor growth and spreading. Semin Cancer Biol 15: 300-308, 2005.
11. Dombrauckas JD, Santarsiero BD and Mesecar AD: Structural basis for tumor pyruvate kinase M2 allosteric regulation and catalysis. Biochemistry 44: 9417-9429, 2005.
12. Li YH, Li XF, Liu JT, Wang H, Fan LL, Li J and Sun GP: PKM2, a potential target for regulating cancer. Gene 668: 48-53, 2018.
13. Lv L, Li D, Zhao D, Lin R, Chu Y, Zhang H, Zha Z, Liu Y, Li Z, Xu Y, *et al*: Acetylation targets the M2 isoform of pyruvate kinase for degradation through chaperone-mediated autophagy and promotes tumor growth. Mol Cell 42: 719-730, 2011.
14. Livak KJ and Schmittgen TD: Analysis of relative gene expression data using real-time quantitative PCR and the 2(-Delta Delta C(T)) method. Methods 25: 402-408, 2001.
15. Zhang S, Hu B, You Y, Yang Z, Liu L, Tang H, Bao W, Guan Y and Shen X: Sorting nexin 10 acts as a tumor suppressor in tumorigenesis and progression of colorectal cancer through regulating chaperone mediated autophagy degradation of $p21^{Cip1/WAF1}$. Cancer Lett 419: 116-127, 2018.
16. Arias E and Cuervo AM: Pros and cons of chaperone-mediated autophagy in cancer biology. Trends Endocrinol Metab 31: 53-66, 2020.
17. Zhang Z, Deng X, Liu Y, Liu Y, Sun L and Chen F: PKM2, function and expression and regulation. Cell Biosci 9: 52, 2019.
18. Zhang J, Feng G, Bao G, Xu G, Sun Y, Li W, Wang L, Chen J, Jin H and Cui Z: Nuclear translocation of PKM2 modulates astrocyte proliferation via p27 and -catenin pathway after spinal cord injury. Cell Cycle 14: 2609-2618, 2015.
19. Azoitei N, Becher A, Steinestel K, Rouhi A, Diepold K, Genze F, Simmet T and Seufferlein T: PKM2 promotes tumor angiogenesis by regulating HIF-1α through NF-κB activation. Mol Cancer 15: 3, 2016.
20. de Wit RH, Mujić-Delić A, van Senten JR, Fraile-Ramos A, Siderius M and Smit MJ: Human cytomegalovirus encoded chemokine receptor US28 activates the HIF-1α/PKM2 axis in glioblastoma cells. Oncotarget 7: 67966-67985, 2016.
21. Peng JQ, Han SM, Chen ZH, Yang J, Pei YQ, Bao C, Qiao L, Chen WQ and Liu B: Chaperone-mediated autophagy regulates apoptosis and the proliferation of colon carcinoma cells. Biochem Biophys Res Commun 522: 348-354, 2020.
22. Liang J, Cao R, Wang X, Zhang Y, Wang P, Gao H, Li C, Yang F, Zeng R, Wei P, *et al*: Mitochondrial PKM2 regulates oxidative stress-induced apoptosis by stabilizing Bcl2. Cell Res 27: 329-351, 2017.
23. Lu WQ, Hu YY, Lin XP and Fan W: Knockdown of PKM2 and GLS1 expression can significantly reverse oxaliplatin-resistance in colorectal cancer cells. Oncotarget 8: 44171-44185, 2017.
24. Yuan S, Qiao T, Zhuang X, Chen W, Xing N and Zhang Q: Knockdown of the M2 isoform of pyruvate kinase (PKM2) with shRNA enhances the effect of docetaxel in human NSCLC cell lines in vitro. Yonsei Med J 57: 1312-1323, 2016.
25. Gorantla NV and Chinnathambi S: Autophagic pathways to clear the tau aggregates in Alzheimer's disease. Cell Mol Neurobiol 41: 1175-1181, 2021.